



One-Pot Synthesis Green Zinc Oxide Nanoparticles immobilized on Activated Carbon derived from Pineapple Peel for Adsorption of Pb(II)

Vienna Saraswaty

Research Centre for Applied Microbiology, National Research and Innovation Agency Republic of Indonesia, KST Samaun Sa-madikun, Bandung 40135, Indonesia, vien001@brin.go.id

Evyka Setya Aji

Research Centre for Applied Microbiology, National Research and Innovation Agency Republic of Indonesia, KST Samaun Sa-madikun, Bandung 40135, Indonesia

Ardi Ardiansyah

Research Centre for Applied Microbiology, National Research and Innovation Agency Republic of Indonesia, KST Samaun Sa-madikun, Bandung 40135, Indonesia

Ayu Hanifah

Research Centre for Applied Microbiology, National Research and Innovation Agency Republic of Indonesia, KST Samaun Sa-madikun, Bandung 40135, Indonesia

Nathania Puspitasari

Department of Chemical Engineering, Widya Mandala Surabaya Catholic University, Kalijudan 37, Surabaya, 60114, Indonesia

See next page for additional authors

Follow this and additional works at: <https://kijoms.uokerbala.edu.iq/home>

 Part of the [Biology Commons](#), and the [Chemistry Commons](#)

Recommended Citation

Saraswaty, Vienna; Aji, Evyka Setya; Ardiansyah, Ardi; Hanifah, Ayu; Puspitasari, Nathania; Santoso, Shella Permatasari; Hartono, Sandy Budi; Risdian, Chandra; Chaldun, Elsy Rahimi; and Setiyanto, Henry (2024) "One-Pot Synthesis Green Zinc Oxide Nanoparticles immobilized on Activated Carbon derived from Pineapple Peel for Adsorption of Pb(II)," *Karbala International Journal of Modern Science*: Vol. 10 : Iss. 2 , Article 1.

Available at: <https://doi.org/10.33640/2405-609X.3347>

This Research Paper is brought to you for free and open access by Karbala International Journal of Modern Science. It has been accepted for inclusion in Karbala International Journal of Modern Science by an authorized editor of Karbala International Journal of Modern Science. For more information, please contact abdulateef1962@gmail.com.

One-Pot Synthesis Green Zinc Oxide Nanoparticles immobilized on Activated Carbon derived from Pineapple Peel for Adsorption of Pb(II)

Abstract

The current study introduces a one-pot technique for synthesizing an environmentally benign and cheap composite adsorbent, namely ZnO-PPAC, for the adsorption of Pb(II). The designated adsorbent was prepared by incorporating green synthesized zinc oxide (ZnO) nanoparticles on activated carbon-derived from pineapple peel. The prepared adsorbents were characterized using XRD, SEM, EDS, FTIR, and BET techniques. The XRD pattern verifies that the ZnO was successfully synthesized and immobilized onto the PPAC in a one pot synthesis system. The surface areas of ZnO-PPAC and PPAC adsorbents were 13.62 m²/g and 961.96 m²/g, respectively. The FTIR evaluation of the ZnO-PPAC adsorbent revealed several characteristic absorption peaks corresponding to -OH groups, C-O groups, C=C groups, C-N groups, and M-O groups. It was revealed that the adsorption of Pb(II) on the ZnO/PPAC adsorbent would not require any pH adjustment. The adsorption kinetics demonstrated that the adsorption of Pb(II) ions on PPAC and ZnO-PPAC better fitted pseudo-second-order kinetics ($R^2 = 0.999$, both for PPAC and ZnO/PPAC) and followed the Freundlich model ($R^2 = 0.989$ and 0.987 for PPAC and ZnO/PPAC adsorbent). According to the Freundlich model, the adsorption of Pb(II) ions onto the designated adsorbents involves a multilayer process. The maximum adsorption capacities of ZnO/PPAC and PPAC were calculated as 769 mg/g and 667 mg/g, respectively. Thermodynamic analysis indicated an exothermic and spontaneous nature, as suggested by the negative values of ΔH° and ΔG° . In summary, both the prepared adsorbents greatly exhibited a high adsorption capacity of Pb(II) ions that can be used for environmental remediation.

Keywords

Adsorbent; green; Nanoparticles; pineapple peel; zinc oxide

Creative Commons License



This work is licensed under a [Creative Commons Attribution-Noncommercial-No Derivative Works 4.0 License](https://creativecommons.org/licenses/by-nc-nd/4.0/).

Authors

Vienna Saraswaty, Evyka Setya Aji, Ardi Ardiansyah, Ayu Hanifah, Nathania Puspitasari, Shella Permatasari Santoso, Sandy Budi Hartono, Chandra Risdian, Elsy Rahimi Chaldun, and Henry Setiyanto

RESEARCH PAPER

One Pot Synthesis Green Zinc Oxide Nanoparticles Immobilized on Activated Carbon Derived from Pineapple Peel for Adsorption of Pb(II)

Vienna Saraswaty^{a,b,**}, Evyka S. Aji^a, Ardi Ardiansyah^a, Ayu Hanifah^a,
Nathania Puspitasari^{c,b}, Shella P. Santoso^{c,b}, Sandy B. Hartono^{c,b}, Chandra Risdian^{a,b},
Elsy R. Chaldun^d, Henry Setiyanto^{e,*}

^a Research Centre for Applied Microbiology, National Research and Innovation Agency Republic of Indonesia, KST Samaun Samadikun, Bandung, 40135, Indonesia

^b Collaborative Research Center for Zero Waste and Sustainability, Jl. Kalijudan 37, Surabaya, 60114, Indonesia

^c Department of Chemical Engineering, Widya Mandala Surabaya Catholic University, Kalijudan 37, Surabaya, 60114, Indonesia

^d Research Center for Environmental and Clean Technology, National Research and Innovation Agency, Kawasan Puspiptek Gedung 820, Tangerang Selatan, 15314, Indonesia

^e Analytical Chemistry Research Group, Institut Teknologi Bandung, Jl. Ganesha 10, Bandung, 40132, Indonesia

Abstract

The current study introduces a one-pot technique for synthesizing an environmentally benign and cheap composite adsorbent, namely ZnO-PPAC, for the adsorption of Pb(II). The designated adsorbent was prepared by incorporating green synthesized zinc oxide (ZnO) nanoparticles on activated carbon-derived from pineapple peel. The prepared adsorbents were characterized using XRD, SEM, EDS, FTIR, and BET techniques. The XRD pattern verifies that the ZnO was successfully synthesized and immobilized onto the PPAC in a one pot synthesis system. The surface areas of ZnO-PPAC and PPAC adsorbents were 13.62 m²/g and 961.96 m²/g, respectively. The FTIR evaluation of the ZnO-PPAC adsorbent revealed several characteristic absorption peaks corresponding to –OH groups, C–O groups, C=C groups, C–N groups, and M–O groups. It was revealed that the adsorption of Pb(II) on the ZnO/PPAC adsorbent would not require any pH adjustment. The adsorption kinetics demonstrated that the adsorption of Pb(II) ions on PPAC and ZnO-PPAC better fitted pseudo-second-order kinetics ($R^2 = 0.999$, both for PPAC and ZnO/PPAC) and followed the Freundlich model ($R^2 = 0.989$ and 0.987 for PPAC and ZnO/PPAC adsorbent). According to the Freundlich model, it is suggested that the adsorption of Pb(II) ions onto the designated adsorbents involves a multilayer process. The maximum adsorption capacities of ZnO/PPAC and PPAC were calculated as 769 mg/g and 667 mg/g, respectively. Thermodynamic analysis indicated an exothermic and spontaneous nature, as suggested by the negative values of ΔH° and ΔG° . In summary, both the prepared adsorbents greatly exhibited a high adsorption capacity of Pb(II) ions that can be used for environmental remediation.

Keywords: Adsorbent, Green, Nanoparticles, Pineapple peel, Zinc oxide

1. Introduction

Metals with a density of not less than 5.3 g/cm³ are classified as heavy metals. In comparison to light metals, heavy metals are less reactive and less soluble in their sulfide or hydroxide form.

According to the density characteristic, some metals, such as arsenic, cadmium (Cd), chromium (Cr), lead (Pb), and mercury (Hg), are considered heavy metals [1,2]. The high frequency of industrial activities such as metal mining [3], lead-based paint [4], battery production [5,6], automobiles [7,8], and

Received 27 December 2023; revised 19 March 2024; accepted 22 March 2024.
Available online 18 April 2024

* Corresponding author.

** Corresponding author at: Research Centre for Applied Microbiology, National Research and Innovation Agency Republic of Indonesia, KST Samaun Samadikun, Bandung, 40135, Indonesia.

E-mail addresses: vien001@brin.go.id (V. Saraswaty), setiyanto@itb.ac.id (H. Setiyanto).

<https://doi.org/10.33640/2405-609X.3347>

2405-609X/© 2024 University of Kerbala. This is an open access article under the CC-BY-NC-ND license (<http://creativecommons.org/licenses/by-nc-nd/4.0/>).

electroplating [9,10], as well as acid rain, chemical fertilizers, pesticides, and sewage, can introduce those metals into the environment. To limit the presence of heavy metals in the environment and maintain environmental sustainability, the Indonesian government has issued a national quality standard under Regulation No. 22/2021 about the limit of heavy metals allowed in water. In that regulation, the water designated for drinking water, water cultivation, fisheries, irrigation and livestock should have heavy metal concentrations below 0.01, 0.03, and 0.05 mg/L, for Cd, Pb, and Cr, respectively [11]. This regulation is required because a large amount of heavy metals accumulation can be harmful to humans and the environment. In humans, heavy metals have the tendency to have negative health effects [1,12]. A study has shown that there is a correlation between high urinary Pb concentration in workers with high diastolic blood pressure or hypertension. In addition, people with cardiovascular disease show higher absorption of heavy metals than healthy people due to the reduction of adenosine triphosphate enzyme activity and stimulation of Ca/Na pumping [13]. It is also reported that patients with high Pb concentrations in their blood tend to have kidney stones [14]. The high concentration of Pb in humans is possible from a Pb-contaminated environment or food.

Removal of heavy metals from environments can be performed by applying several chemical [15], physical [16–18], and biological [19,20] treatments. The advantages of applying chemical treatment are easy operation, less expensive, broad applications, less sludge quantity, easier dehydration, and efficiency for the elimination of several heavy metals. However, the methods also have limitations, such as being problematic for dewatering and disposal, not suitable for wastewaters with high concentrations of heavy metals, and that metallic sulfide precipitation is less and not stable. In addition, some chemical precipitation methods require high temperatures and energy consumption. Biological treatment has shown a promising way of treating heavy metals [21,22]. The microorganisms used in biological treatments immobilize the molecular structure of heavy metals, resulting in partial mineralization or transmutation. Unfortunately, due to limitations to the environmental condition as well as the requirements of nutrients for bacterial growth, biological treatments are not universally preferred [23]. The physical treatment of adsorption is frequently used for treating metal-contaminated water; this method can be used to treat low to high concentrations of metal contamination [24–28]. More importantly, compared to more complex methods

such as electrolysis or ion exchange, adsorption is simple and less expensive.

Because of their cost effectiveness and environmentally friendly nature, the use of biomass-derived adsorbents is becoming more popular. However, the low adsorption capacity and affinity of the biomass-derived adsorbent are the shortcomings that need to be improved prior to optimizing the effectiveness and affordability of the process. Biomass waste such as citrus peel [29], pineapple peel (PP) [28,30], corn cob [31,32], rice husk [33,34], wheat straw [35,36], *Aloe vera*, and palm leaves are potential sources of adsorbent because they are abundantly available and inexpensive. Biomass waste may not have a high adsorption capacity if directly used in its original form, which can be improved by converting it into carbon [35,36]. For example: the maximum adsorption capacity of methylene blue on the original banana peel adsorbent was about 25 mg/g; when the banana peels were converted into carbon, the maximum adsorption capacity improved 13-fold, which is equal to 333 mg/g [37]. Additionally, activated carbon derived from *A. vera* leaves could adsorb ~90% of phenolic compounds (bisphenol A and pentachlorophenol) at 40 mg/L from wastewater at an adsorbent dose of 4.2 g/L [38]. In this work, we utilized PP as the source of biomass waste to be converted into carbon due to its abundant availability.

Recent studies have shown an increasing focus on improving the performance of an adsorbent by modifying the surface functional groups [39], hybridizing [40], altering the porosity of the structure of the adsorbent through physicochemical and mechanical treatment [41–44], as well as activating the surface [45,46]. Hybridization using nanoparticles to remove pollutants from wastewater is of interest because nanoparticles have demonstrated good results in the adsorption of both organic and inorganic compounds [47–49]. For example, incorporation of Fe₃O₄ with graphene oxide enhanced the removal efficiency of cefixime. Furthermore, magnetization of activated carbon derived from banana peel and salvia seeds, as well as magnetization of multi-walled carbon nanotubes, exhibited a higher and greater adsorption capacity than that of its origin towards the pollutant tested [50–52]. Those reports suggest that by creating a nanocomposite, carbon sequestration performance can be improved.

Kikuchi et al. (2006) have demonstrated the preparation of an activated carbon-ZnO hybrid adsorbent via immersion of activated carbon in a Zn(II) solution for 7 days [53]. Whereas Pourali et al. (2023) successfully loaded the ZnO nanoparticles on activated carbon derived from worn rubber by

immersing and stirring the ZnO nanoparticles and activated carbon at 500 rpm for 2 h [54]. In those reports, incorporation of ZnO nanoparticles onto the activated carbon improved the adsorption performance [53,54]. Unfortunately, the long-term of indirect impregnation process and separated synthesis of green synthesized ZnO nanoparticles and activated carbon have led to ineffectiveness. To the best of our knowledge, there has been no report regarding the preparation of ZnO immobilized on activated carbon derived from pineapple peel biomass in a one-pot synthesis system. Herein, a simple and fast impregnation of ZnO on activated carbon derived from pineapple peel (ZnO-PPAC) in a one-pot system is being demonstrated in this work. The designated adsorbents were characterized employing several techniques, such as fourier-transform infra-red (FTIR), X-ray diffraction analysis (XRD), specific surface area and pore size calculation using the BET model, and surface morphology analysis using a scanning electron microscope (SEM) in conjunction with EDS. The adsorption performance of prepared adsorbents was further analyzed by employing a synthetic solution containing Pb(II) ions. The analyses encompassed thermodynamic aspects, equilibrium conditions, kinetic behavior, and alterations in pH adjustment.

2. Materials and methods

2.1. Chemicals

The chemicals used in this study are sodium hydroxide (NaOH, 99% purity, eMerck), lead ion stock solution (1000 mg/L, eMerck), zinc nitrate ($\text{ZnNO}_3 \cdot 12\text{H}_2\text{O}$), 99%, eMerck), and hydrochloric acid 37% (HCl, eMerck). Pineapple peels (PP) were purchased from a local market located in Subang, West Java, Indonesia. All chemicals were employed without further purification, and the solutions were prepared in aqua demineral (aqua DM). HCl or NaOH at 0.2 M was employed to adjust the pH of solutions.

2.2. Preparation of PPAC adsorbent

About 50 g of pineapple peel powder was macerated in 500 mL of aquadest, and the pH of the solution was adjusted to 12.0 by introducing a 2M NaOH solution. The process was allowed for 4 h at 80 °C. Subsequently, the solid was collected via centrifugation (3000 rpm, 15 min) and rinsed with aqua DM until the pH of the solution reached neutral. The residues were collected in a falcon tube

and dehydrated in an oven at 80 °C overnight. The residues were then placed in a closed crucible and carbonized in a furnace (400 °C, 2 h). The obtained adsorbent was denoted as PPAC and kept in desiccators prior to analysis.

2.3. Preparation of ZnO nanoparticles derived from PP extract

ZnO nanoparticles were synthesized by utilizing PP extract. Prior to the synthesis of ZnO, the precursor salt, ($\text{Zn}(\text{NO}_3)_2$), was dissolved in aqua demineral (1 mg/mL). Meanwhile, PP extract was prepared freshly by macerating 20 gr of PP powder in 400 mL of aqua DM and heating at 60 °C for 30 min. After maceration, the supernatant and biomass were separated by means of centrifugation (3000 rpm, 20 min). 20 mL of supernatant was added slowly into the prepared 20 mL of Zn solution and stirred at room temperature (200 rpm, 15 min). The pH of the reaction was raised to 12.0 by introducing 0.2 M NaOH, and the reaction was continuously agitated for 2 h at 80 °C. The white precipitates were collected by centrifugation (3000 rpm, 20 min), and then rinsed until the pH of the supernatant reached 7. The solid was then dehydrated at 80 °C for overnight, then calcined (400 °C, 2 h). The obtained ZnO was then kept in desiccators for further analysis.

2.4. Preparation of ZnO/PPAC composite adsorbent

The ZnO-PPAC composite adsorbent was prepared by combining the PPAC and ZnO preparation procedures in a one-pot synthesis system. Specifically, 0.1 g of zinc nitrate was dissolved separately in 10 mL of aqua DM. About 10 g of PP powder was macerated in 200 mL aqua DM and heated at 60 °C for 30 min. Next, the zinc salt solution was slowly poured into the macerated PP. In this process, the biomass of PP was not separated. The mixture was then constantly stirred for 15 min at an agitation speed of 200 rpm and a temperature of 80 °C, and the pH of the solution was adjusted to 12 by adding several drops of NaOH 2M. After pH adjustment, the process was continued for 2 h at 80 °C. The solids were washed with aqua DM for a minimum of three times and until the pH of the supernatant reached neutral. The solids were collected via centrifugation (3000 rpm, 20 min). The obtained composite was dehydrated in an oven at 80 °C overnight prior to calcination (400 °C, 2 h). After calcination, the obtained solid was denoted as ZnO/PPAC and kept in a desiccator prior to evaluation.

2.5. Characterization

The X-ray diffraction (XRD) pattern was recorded employing a Bruker D8 Advance instrument with Cu-K α radiation at λ of 1.54 Å and a scan rate of 0.04 2 θ /s for 2 θ ranging from 10° to 80°. Fourier transform infrared (FTIR) analysis was analyzed using a Nicolet i5. The FTIR measurement was recorded at a wavenumber of 400–4000 cm⁻¹. Scanning electron microscopy-energy dispersive spectroscopy (SEM-EDS) characterization was observed using a JEOL IT-300. The specific surface area and pore volume were calculated using N₂ sorption-desorption measurements in a Quantachrome NOVA instrument.

2.6. Batch adsorption experiment

The batch adsorption experiment was performed to determine the adsorption capacity, thermodynamic, kinetic, and isotherm models of Pb(II) ions. A stock solution of Pb(II) ions at 1000 mg/L was prepared by dissolving 1000 mg of PbO in aqua DM with the addition of HCl. The Pb(II) stock solution was freshly prepared prior to analysis. All the adsorption experiments were performed triplicate. For the kinetic study, the solution of Pb(II) at concentrations of 500 mg/L and 100 mg/L was prepared by diluting the Pb(II) ions stock solution. The adsorbents were tested at a dose of 1 g/L (m/V) and agitated at 150 rpm at room temperature. The supernatants were collected at a time interval of 0.5–30 min. The effects of several parameters such as pH (2–8), initial Pb(II) concentration (20–500 mg/L), and temperature (298–313 K) were investigated under the following conditions: agitation speed: 150 rpm, room temperature, adsorbent dose of 30 mg for 30 mL of 500 mg/L Pb(II) solution, and 30 min of contact time. The samples were collected individually, and the test was performed three times. The concentrations of Pb(II) in the collected samples were determined using atomic absorption spectroscopy (AAS) analysis on a Flame AAS instrument (Shimadzu, ASC-7000). The % removal and adsorption capacity (q_e , mg/g) were determined using Equations (1) and (2), respectively.

$$\% \text{ Removal} = \frac{C_0 - C_e}{C_0} \times 100 \% \quad (1)$$

$$q_e = \frac{C_0 - C_e}{m} \times V \quad (2)$$

where C_e and C_0 (mg/L) reflect the equilibrium and initial Pb(II) concentrations, respectively; q_e (mg/g) denotes the amount of Pb(II) removed at equilibrium; V is the volume of the Pb(II) solution (L); and

m is the weight of the adsorbent used (g) [53]. The results were analyzed by simulation of kinetic models, thermodynamic studies, and isotherm studies (Langmuir and Freundlich).

3. Results and discussion

3.1. X-ray diffraction analysis

Fig. 1a shows the recorded XRD pattern from ZnO particles derived PP extract. Several prominent peaks were observed at 2 θ of 31.6°, 34.2°, 36.1°, 47.3°, 56.4°, and 62.7°; these peaks are well matched with reported JCPDS number 36–1451 for hexagonal wurtzite ZnO nanoparticles, corresponding to crystal planes (100), (002), (101), (102), (110), and (103) respectively. Calculation of the crystalline domain size of ZnO using the Debye–Scherrer equation results in an average crystal size of 57 nm, which is larger than reported (i.e., 15–41 nm) [55,56]. This can be attributed to the variation in operating conditions, including the type of precursor, reaction temperature, and time, as revealed previously [55]. Several characteristic peaks of ZnO particles appeared in the XRD pattern of the ZnO/PPAC adsorbent (Fig. 1b). Specifically, the peak corresponds to the ZnO crystal plane (100), (002), (101), (102), (110), and (103) at 2 θ of 31.6°, 34.2°, 36.1°, 47.3°, and 56.4°. However, those peaks exhibit a lower intensity, which can be attributed to the decrease in crystallinity following the hybridization of ZnO with low-crystallinity PPAC. The calculated average crystal size of ZnO in the ZnO-PPAC adsorbent was found to be 44 nm. Fig. 1c shows the XRD pattern of PPAC. As presented in Fig. 1c, the peak characteristic of ZnO was not observed in the XRD pattern of PPAC. At the same time, the XRD pattern of the PPAC adsorbent obviously detects the presence of some crystal materials that are Ca(OH)₂, CaCO₃, and SiO₂. It seems calcium carbazide, which is widely used for fruit ripening, results in the

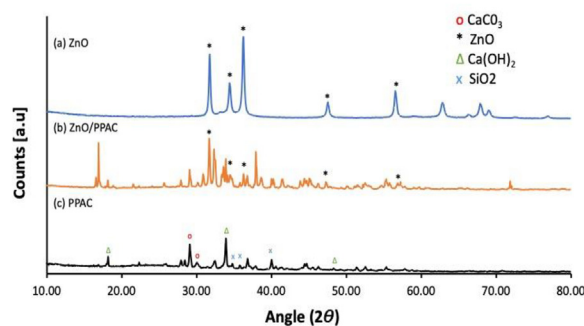


Fig. 1. XRD pattern of the (a) ZnO-derived PP, (b) ZnO/PPAC, and (c) PPAC adsorbents.

presence of Ca-molecules in PPAC. Specifically, the reaction of calcium carbazide results in the formation of $\text{Ca}(\text{OH})_2$. Since the preparation of the PP powder was performed in an open compartment, it is possible for $\text{Ca}(\text{OH})_2$ to interact with carbon dioxide in the air, then form CaCO_3 .

3.2. Scanning electron microscopy analysis

Fig. 2a shows the surface morphology of the ZnO nanoparticles derived from PP extract. The ZnO nanoparticles appear to be agglomerated and have heterogenous shapes. Some of the ZnO particles appeared to have rod-like shapes, and some had flower-like shapes. The use of PP extract for the green synthesis of ZnO results in heterogeneous-shaped ZnO, which is like the previously synthesized ZnO from *Elaeagnus angustifolia* L. leaf extract [57]. Fig. 2b shows that the PPAC adsorbent has grid, porous, and dense morphology. The presence of pores in PPAC suggests their potency as an effective adsorbent. The presence of ZnO on the PPAC is later confirmed in Fig. 2c. As illustrated, the ZnO nanoparticles are denoted with yellow arrows; the ZnO nanoparticles appear to be

aggregated and distributed unevenly on PPAC. The presence of ZnO nanoparticles could be mainly responsible for the enhancement of the ZnO-PPAC textural, with regards to its microstructure [58]. The energy dispersive spectroscopy (EDS) evaluation corroborated the presence of the ZnO attached to the PPAC because the PPAC adsorbent did not show the presence of the Zn element (see Fig. 3a–c). The EDS evaluation of PPAC displays that the PPAC adsorbent contains C, O, Ca, Na, and Si elements, that mutually support the XRD analysis.

3.3. FTIR evaluation

Fig. 4 illustrates the FTIR spectra of ZnO, PPAC, as well as ZnO-PPAC. The ZnO derived from PP extract shows a peak at 847 cm^{-1} , which corresponds to C–H bending of aromatics; peaks at 1057 and 1015 cm^{-1} , which relate to C–N stretching of amines; a peak at 1558 cm^{-1} , which relates to CH bending of alkanes; a peak at 3449 cm^{-1} , which relates to O–H stretching of polyphenols; and the typical metal–oxygen peak at 546 cm^{-1} , which corresponds to Zn–O. The combination of C–

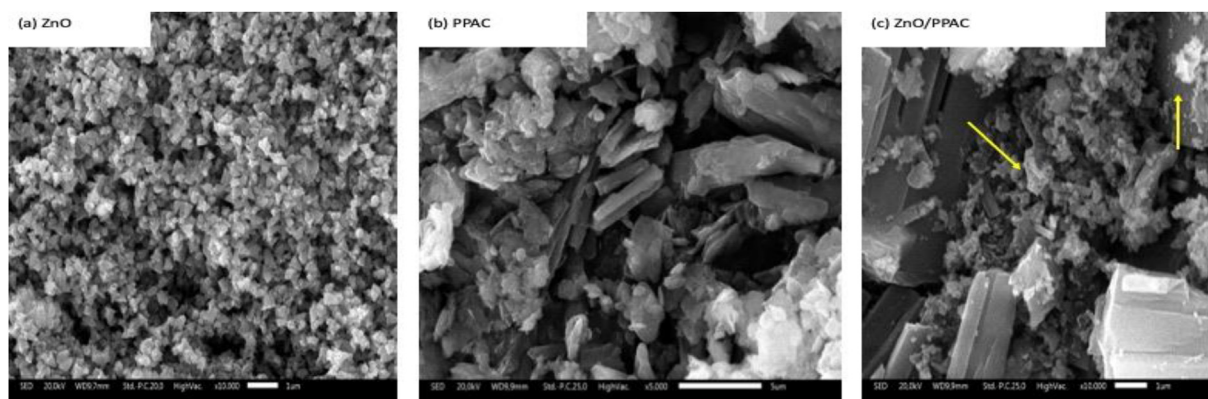


Fig. 2. SEM images of the (a) ZnO-derived PP, (b) PPAC, and (c) ZnO/PPAC adsorbents.

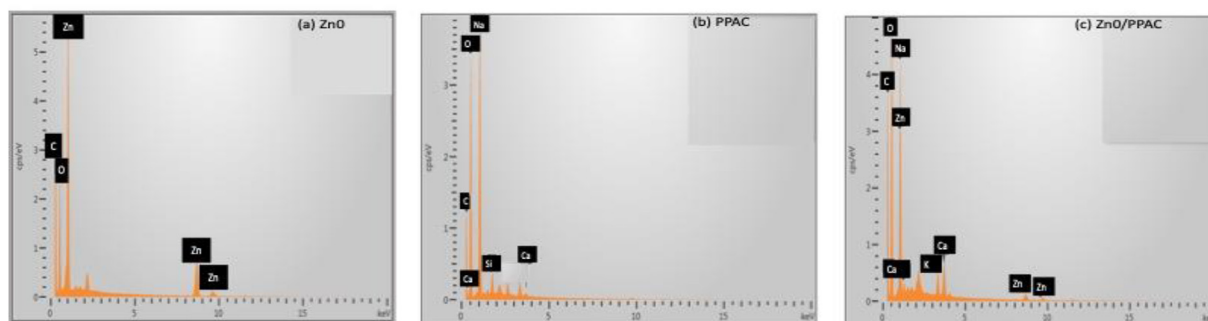


Fig. 3. EDS spectrum of the (a) ZnO-derived PP, (b) PPAC, and (c) ZnO/PPAC adsorbents.

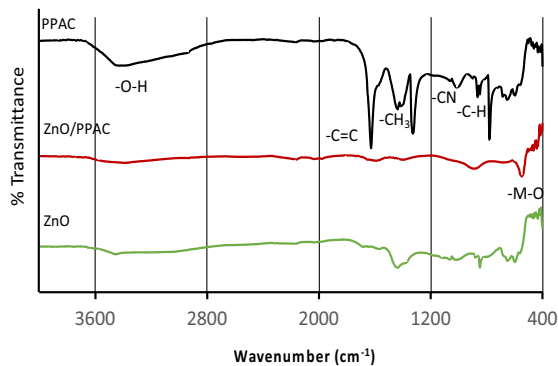


Fig. 4. FTIR spectra of ZnO derived PP, ZnO/PPAC, and PPAC adsorbents.

containing groups with OH- groups can contribute to the presence of polyphenols originating from PP extract. The FTIR spectrum of PPAC exhibits a strong peak at 1625 cm^{-1} correlated to the C=C stretching vibration. Other peaks related to the C-containing groups were also appearing as intense peaks, indicating the high carbon content of PPAC after the carbonization process. Next, the FTIR spectrum of ZnO/PPAC was further compared to the FTIR spectrum of PPAC. In the FTIR spectrum of ZnO-PPAC, the peaks of PPAC at 3427 , 1438 , and 1325 cm^{-1} appeared to shift to 3382 , 1577 , and 1396 cm^{-1} . More importantly, the peaks at 1057 cm^{-1} and 1012 cm^{-1} completely disappeared. It is also displayed that the peaks correlated to the C-containing groups appear weaker in ZnO-PPAC, which can be attributed to the decrease in carbon content when the PPAC adsorbent was incorporated with ZnO nanoparticles.

3.4. Surface area calculation

The surface area measurement is essential in recognizing the characteristics of an adsorbent. The N_2 adsorption–desorption isotherm evaluation using the BET model was used to figure out the surface areas of ZnO/PPAC and PPAC adsorbents. As shown in Table 1, the incorporation of ZnO nanoparticles onto PPAC decreased both the pore volume and specific surface area. It seems the aggregation of ZnO nanoparticles on the PPAC and the impregnation of ZnO into the pores present at

Table 1. Surface area and pore volume of PPAC and ZnO/PPAC adsorbent.

Adsorbent	Surface area (m^2/g)	Pore volume (cm^3/g)
PPAC	961.96	3.292
ZnO/PPAC	13.62	0.029

the PPAC, as suggested in the SEM image, accounted for this.

3.5. Kinetic study

The effects of contact time on the removal of Pb(II) ions using the PPAC and ZnO/PPAC composite adsorbents were examined. The evaluations apply 30 mg of adsorbent and 30 mL of Pb(II) ions at concentrations of 100 mg/L and 500 mg/L. As demonstrated in Fig. 5, the kinetic study revealed a clear association between the increment in contact time and the quantity of Pb(II) removed. Upon extending the contact time from 5 to 30 min, the quantity of Pb(II) attached to the adsorbent rose slowly after an initial rapid adsorption in the first 0.5 min. This can be explained as follows: During the beginning of the adsorption process, the sites were initially free or unoccupied and therefore had a high affinity for Pb(II) ions, leading to quick adsorption. As the adsorption progressed, the adsorption sites reached saturation, resulting in stagnation in the removal of Pb(II) ions. The effect of contact time was also evaluated at different initial concentrations of Pb(II) ions. It is evident that the adsorption process was faster when the starting concentration of Pb(II) was higher than 100 mg/L. It seems the higher Pb(II) concentration results in a stronger force to encounter the mass transfer gradient, as the impact causes faster adsorption. At equilibrium conditions, however, the initial concentration of Pb(II) does not have a significant effect, especially for the ZnO-PPAC adsorbent. Thus, the optimum equilibrium time was determined to be 5 min for the ZnO-PPAC adsorbent and 10 min for the PPAC adsorbent.

To understand the separation mechanism of Pb(II) on the designated adsorbent, the kinetics of Pb(II) adsorption were further analyzed. For that purpose, kinetic equations that are pseudo first and pseudo second order, Equations (3) and (4) were used, respectively.

$$\log(q_e - qt) = \log q_e - \frac{k_1}{2.303}t \quad (3)$$

$$\frac{1}{qt} = \frac{1}{k_2 \cdot qe^2} - \frac{1}{qe}t \quad (4)$$

The parameters qt and qe represent the quantity of Pb(II) ions attached to the PPAC and ZnO/PPAC adsorbent at a specific time point and equilibrium, respectively. The k_1 and k_2 correspond to the rate constants of pseudo-first and pseudo-second order, respectively. Fig. 6(a-d) displays the relationship between $\log(qe-qt)$ vs t as well as t/qt vs

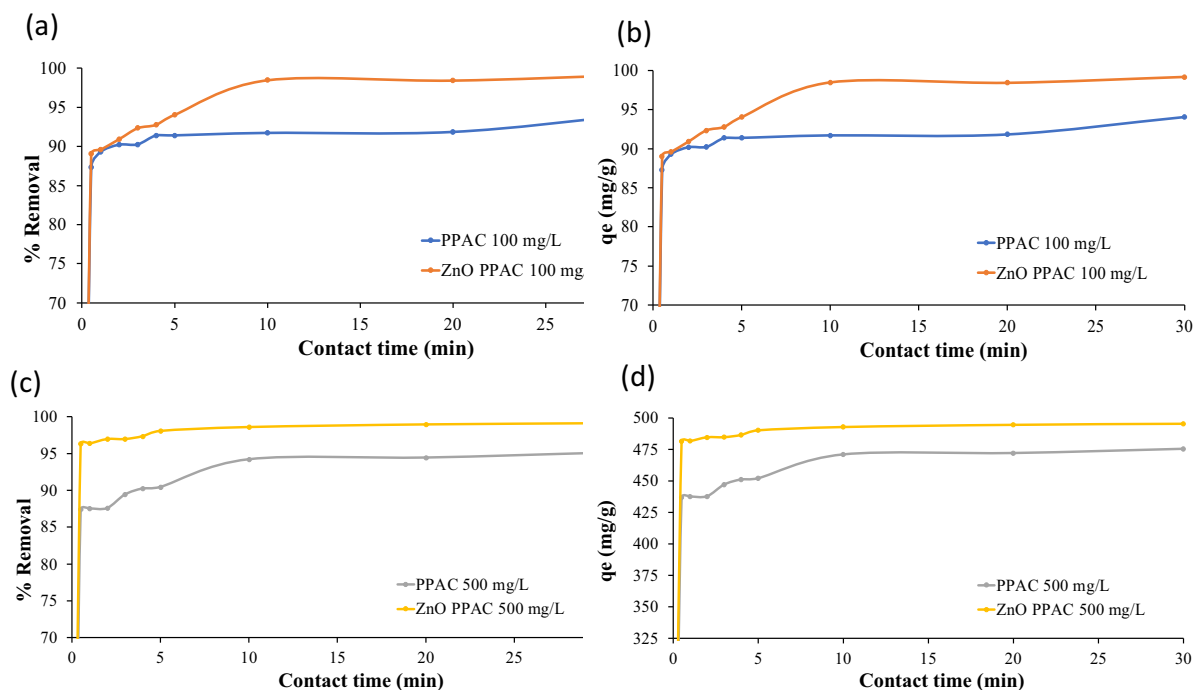


Fig. 5. Effect of contact time on the % removal of 500 mg/L Pb(II) ions (a–c) and adsorption capacity (b–d) at PPAC and ZnO/PPAC adsorbents (condition: adsorbent dose 30 mg/30 mL, agitation speed 200 rpm, room temperature, initial Pb(II) concentration 100 mg/L and 500 mg/L, contact time: 0.5–30 min).

t for the adsorption of Pb(II) ions on PPAC and ZnO-PPAC adsorbents. Table 2 features the list of parameters of the kinetic models used in this investigation. The fitting using pseudo-first order does not satisfy the experimental data, which reflects the low R^2 value. On the contrary, the fitting using pseudo-second order results in an R^2 value close to unity (R^2 value of 0.999), suggesting a strong relationship between the model and the actual data points. Additionally, the high R^2 value confirmed that the adsorption process of Pb(II) on the PPAC and ZnO/PPAC involves the chemisorption process [59]. The k_2 parameter, which corresponds to the adsorption rate, indicates that the ZnO/PPAC adsorbent has a faster adsorption rate than the PPAC adsorbent when utilized to eliminate Pb(II) at a concentration of 500 mg/L, confirming the benefit of immobilizing of ZnO onto the PPAC.

3.6. The effect of pH

The effect of pH on the elimination of Pb(II) ions using PPAC and ZnO/PPAC adsorbent was analyzed by contacting 30 mg of the designated adsorbent with 30 mL of 500 mg/L of Pb(II) solutions with pH ranging from 2 to 8 for 30 min. The adsorption capacity of Pb(II) at various pHs on

PPAC and ZnO/PPAC adsorbents is illustrated in Fig. 7a. The % removal of Pb(II) by PPAC appeared to increase with the increment of pH from 2 to 5, that is, from 88% to 94%. The % removal of Pb(II) by PPAC reached its maximum at a pH of 5. The decrease in % removal was observed as the pH was increased over pH 6. The effect of adsorbent surface charge can be correlated to explain this phenomenon. At acidic pH < 5, the high concentration of H^+ causes the positive surface charge of PPAC, which leads to the repulsion effect with the Pb(II) cations. The adsorption of Pb(II) at a pH of 5 may occur beyond the isoelectric point of the PPAC, where PPAC tends to have a negative surface charge. The different charges between PPAC and Pb(II) provide electrostatic attraction, which facilitates the adsorption. Meanwhile, as the pH of the solution was >5, the high concentration of OH^- can induce the formation of Pb-hydroxide species, which lead to the precipitation of Pb(II). The ZnO/PPAC appears to have stable adsorption performance in all investigated pH ranges, where the % removal of Pb(II) using ZnO-PPAC was maintained at ~97%. Therefore, it is suggested that no pH adjustment was considered necessary when the ZnO/PPAC adsorbent was used for the remediation of highly Pb-contaminated water. It seems the rise in % removal

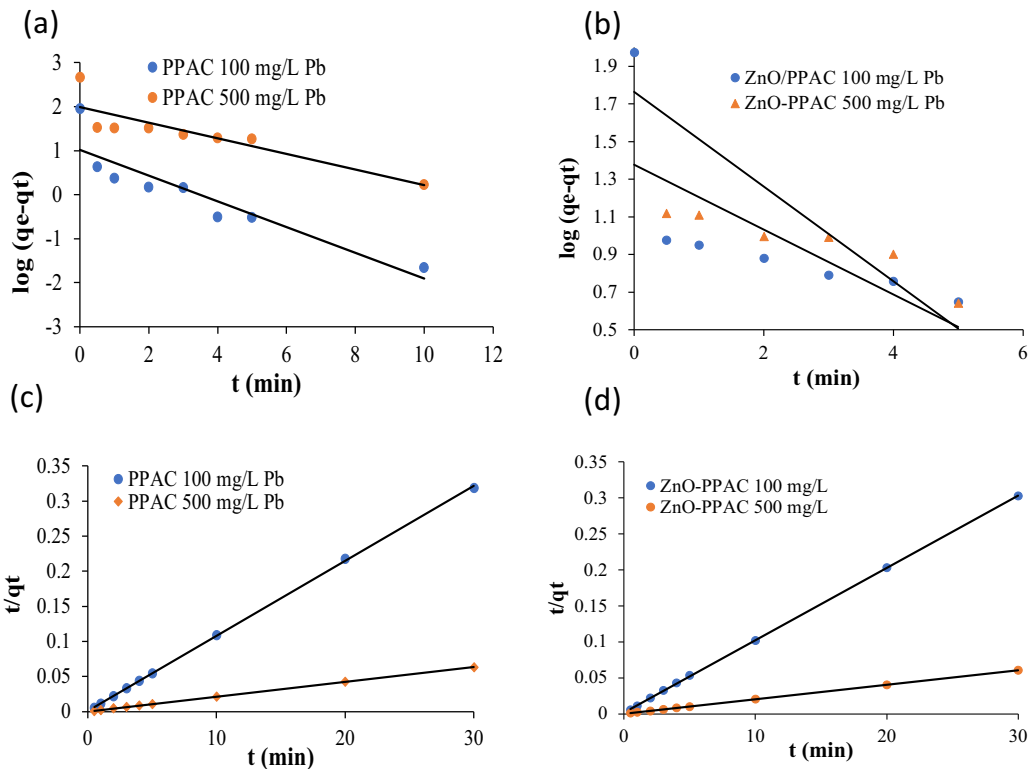


Fig. 6. Pseudo first (a,b) and pseudo second (c,d) order plots for Pb(II) adsorption on PPAC and ZnO-PPAC adsorbents.

of Pb(II) on ZnO/PPAC adsorbent could be associated with the interaction of Pb(II) ions and Pb-hydroxide species with the active sites on the ZnO/PPAC adsorbent's surface through ion exchange or hydrogen bonding mechanisms [60].

Table 2. Kinetics models of the removal mechanism of Pb(II) from solution.

Pseudo-first order kinetic				
C_i (mg/L)	q_e exp (mg/g)	q_e cal. (mg/g)	k_1	R^2
PPAC				
100	94.07	10.39	0.673	0.827
500	475.49	98.51	0.408	0.759
ZnO-PPAC				
100	99.18	58.09	0.579	0.484
500	495.57	23.87	0.397	0.521
Pseudo-second order kinetic				
C_i (mg/L)	q_e exp (mg/g)	q_e cal. (mg/g)	k_2	R^2
PPAC				
100	94.07	95.51	0.102	0.999
500	475.49	475.30	0.0142	0.999
ZnO-PPAC				
100	99.18	100	0.0526	0.999
500	495.57	500	0.0200	0.999

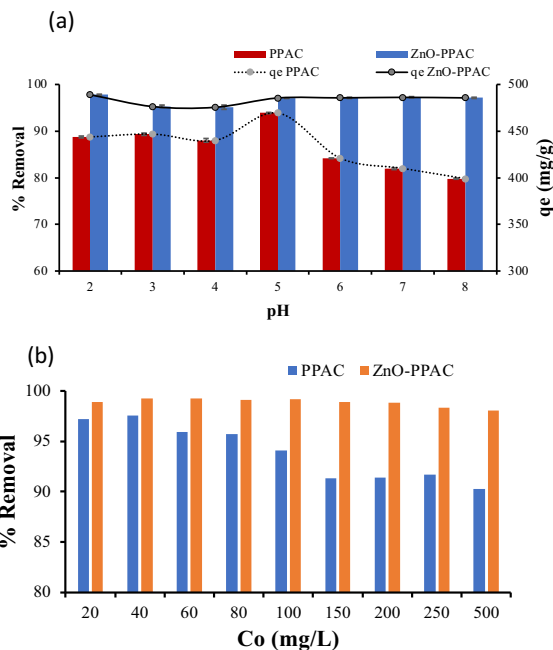


Fig. 7. Effect of pH (a) and initial Pb(II) concentration (b) on the % removal and adsorption capacity of Pb(II) ions at PPAC and ZnO/PPAC adsorbents (condition: adsorbent dose: 30 mg/30 mL of Pb(II) solution) agitation speed: 200 rpm, Room Temperature, contact time: 30 min).

3.7. Equilibrium study

The impacts of the initial Pb(II) concentration (20–500 mg/L) on the % removal efficiency of the PPAC and ZnO/PPAC adsorbent were tested by mixing 30 mg of the prepared adsorbent with 30 mL of Pb(II) solution. As presented in Fig. 7b, when the initial Pb(II) concentration was raised to 60 mg/L, the adsorption of Pb(II) ions on PPAC started to decrease, indicating the beginning of saturation of active sites on the PPAC adsorbent. Meanwhile, the % removal of Pb(II) by ZnO-PPAC does not seem to be affected by the initial concentrations, and the % removal is maintained at over 97% across all initial concentrations tested. This result suggests that ZnO-PPAC possesses a higher number of adsorption sites, so its saturation can be delayed.

The Langmuir and Freundlich models are employed to figure out the adsorption mechanism of Pb(II) ions on the PPAC and ZnO-PPAC adsorbents. The linear expressions of the Langmuir and Freundlich models can be found in Equations (5) and (6), respectively.

$$\frac{C_e}{q_e} = \frac{1}{K_L \cdot q_{\max}} + \frac{C_e}{q_{\max}} \quad (5)$$

$$\text{Log } q_e = \text{Log } K_f + \frac{1}{n} \text{Log } C_e \quad (6)$$

where q_e reflects the quantity of Pb(II) ions that is adsorbed onto ZnO-PPAC or PPAC when the system reaches equilibrium (mg/g) and C_e reflects the concentration of Pb(II) (mg/L) in the solution at equilibrium. The maximum adsorption capacity and Langmuir constants were indicated by q_{\max} and K_L , respectively. The Freundlich constants associated with adsorption capacity are denoted as K_f and $1/n$. The Langmuir model figures out the potential monolayer adsorption mechanism, while the Freundlich model depicts the possibility of multi-layer adsorption. The slope and intercept of the linear plot of C_e/q_e vs. C_e and $\log q_e$ vs. $\log C_e$ (see Fig. 8 a-d) were utilized for determining the Langmuir and Freundlich parameters, and the summaries are tabulated in Table 3.

Table 3. Isotherm parameters for Pb(II) adsorption on PPAC and ZnO/PPAC adsorbents.

Adsorbent	Langmuir			
	q_{\max} (mg/g)	K_L (L/mg)	R_L	R^2
PPAC	667	0.9995	0.002	0.731
ZnO-PPAC	769	1.0003	0.002	0.849
	Freundlich			R^2
	$1/n$	K_f		
PPAC	0.8357	19.015		0.989
ZnO/PPAC	0.7001	104.76		0.987

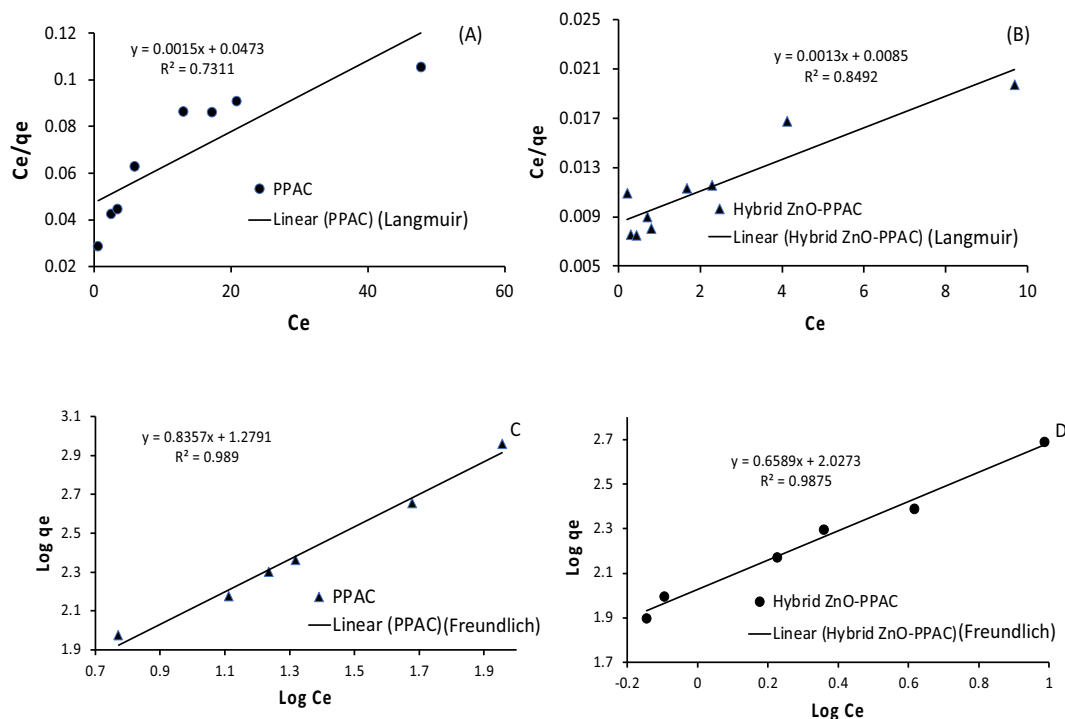


Fig. 8. Langmuir (a,b) and Freundlich (c,d) isotherm models on the separation of Pb(II) ions at PPAC and ZnO-PPAC.

As assessed from the R^2 values in Table 3, the Freundlich model provides a better fit to the experimental data in this study. The suitability of the data points to the Freundlich model indicates the multilayer behavior of the adsorbent. The $1/n$ parameter of the Freundlich model can depict the favorability of the adsorption process, where the adsorption of Pb(II) using PPAC and ZnO-PPAC was found to be favorable as the $1/n$ value is less than 1. The PPAC and ZnO-PPAC exhibited a maximum calculated adsorption capacity (q_{\max}) of approximately 667 and 769 mg/g for Pb(II) ions, respectively. Accordingly, a solution or wastewater that was heavily contaminated with Pb(II) ions could be purified either by PPAC or a ZnO-PPAC adsorbent. By comparing the equilibrium and kinetic evaluations, it was clear that PPAC with impregnated ZnO showed better performance, making it a potential candidate for water treatment applications.

3.8. Thermodynamic study

The effect of temperature on the removal of Pb(II) at the PPAC and ZnO/PPAC adsorbents was investigated at various temperatures ranging from 298 to 333 K. The data were then used for the thermodynamic analysis of Pb(II) on PPAC and ZnO-PPAC adsorbents. Fig. 9 depicts the % removal and adsorption of Pb(II) on the prepared adsorbent. The % removal and adsorption capacity in the experiment were found to decrease as the temperature increased from 298° to 313 K, that is, from 90.30% to 77.3% and 99.1%–79.74% for the adsorption of Pb(II) on PPAC and ZnO-PPAC, respectively. Additionally, an increase in temperature from 313 to 333 K does not cause a significant decrease in the % Pb(II) removal.

The thermodynamic parameters, specifically the change in Gibbs free energy (ΔG°), enthalpy (ΔH°)

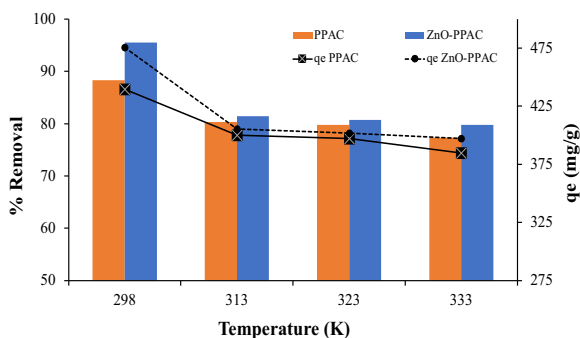


Fig. 9. Adsorption of 500 mg/L Pb(II) ions at PPAC and ZnO/PPAC adsorbents at various temperatures (condition: adsorbent dose 30 mg/30 mL, initial Pb(II) concentration: 500 mg/L, 200 rpm, RT, 30 min contact time).

and entropy (ΔS°) were determined using Equations (7) and (8).

$$\Delta G^\circ = -RT \ln K \quad (7)$$

$$\Delta G^\circ = \Delta H^\circ - T\Delta S^\circ \quad (8)$$

where T is the temperature in Kelvin, R is the universal gas constant ($R = 8.314 \text{ J/mol K}$), and K_c is the thermodynamic equilibrium constant, which is determined from $\ln(q_e/C_e)$. Table 4 summarizes the results of the thermodynamic parameters. As shown, the ΔG° values for PPAC and ZnO-PPAC adsorbents varied from -5.03 to -3.06 kJ/mol . K, whereas ΔG° values for ZnO/PPAC were found in the range from -7.61 to -3.42 kJ/mol . The negative ΔG° values indicate that the adsorption of Pb(II) both on PPAC and ZnO-PPAC adsorbents was spontaneous. This suggests that the Pb(II) ions are adsorbed on the PPAC and ZnO/PPAC without requiring external energy.

Additionally, it is important to highlight that the ΔG° change increased as the temperature rose. Those findings indicated that elevated temperatures do not promote more favorable adsorption. This results in a lower adsorption capacity. The negative values of ΔH° (-18.29 kJ/mol and -39.74 kJ/mol , for PPAC and ZnO/PPAC, respectively) suggest that the adsorption process of Pb(II) on the PPAC and ZnO/PPAC is exothermic in nature. In exothermic adsorption, a high temperature can induce the desorption of the adsorbate, which is due to the bond weakening [61]. The results from thermodynamic evaluation suggest that the adsorption of Pb(II) on the PPAC and ZnO/PPAC adsorbent was more efficient to do at a low temperature.

3.9. Comparative study

The performance of the designated adsorbents in removing Pb(II) ions was compared to other reported low-cost adsorbents. The comparative findings are tabulated in Table 5. Our modified adsorbent surpassed the previously reported

Table 4. Thermodynamic parameters for Pb(II) adsorption on PPAC and ZnO-PPAC adsorbents.

Adsorbent	T(°K)	ΔG° (kJ/mol)	ΔS° (J/mol.K)	ΔH° (kJ/mol)
PPAC	298	-5.03	-45.24	-18.29
	313	-3.52		
	323	-3.42		
	333	-3.06		
ZnO-PPAC	298	-7.61	-110.35	-39.74
	313	-3.69		
	323	-3.57		
	333	-3.42		

Table 5. Adsorption capacity of PPAC, ZnO/PPAC, and other adsorbents for the removal of Pb(II) ions from the literature.

Adsorbent	q _{max} (mg/g)	pH	Ref.
Banana leaves powder/AgNPs	244	6.0	[62]
Bael leaves	104	5.1	[63]
Tamarind wood	134	6.5	[64]
Apricot stone	38.5	6.0	[65]
<i>Citrus limettioides</i> peel carbon	167	4–5	[66]
<i>Citrus limettioides</i> seed carbon	143	4–5	[66]
<i>Phytolacca americana</i> L.	13.2	6.0	[67]
PPAC	667	5	This work
ZnO/PPAC	769	–	This work

adsorbent. The ZnO/PPAC adsorbent seemed to have better performance because of several factors, including electrostatic interactions, the presence of active molecules, multilayer adsorption, and the addition of metal oxide (ZnO) to activated carbon made from biomass.

The advantages of the ZnO/PPAC adsorbent over the PPAC adsorbent include: (1) they do not require pH adjustment when used for the adsorption of Pb(II) ions; (2) the preparation of the modified adsorbent is simple and fast due to the fact that the biomass did not separate during the process; and (3) the greener synthesis process of ZnO produces less waste. Nevertheless, further research is required to explore the economic and sustainable aspects of scaling up the production and use of these adsorbents.

4. Conclusion

In summary, this present work successfully synthesized and characterized a ZnO-PPAC adsorbent that was fabricated in a one-pot synthesis system for the removal of Pb(II) ions. The BET analysis revealed that the surface area of ZnO-PPAC was 13.62 m²/g. The immobilization of ZnO onto the PPAC can introduce an additional active group and enhance the Pb(II) ion adsorption effectiveness. The maximum adsorption capacity of ZnO-PPAC for Pb(II) ions was found to be greater than that of PPAC, as suggested by the q_{max} values of 769 mg/g and 667 mg/g, for ZnO/PPAC and PPAC, respectively, following the Freundlich adsorption isotherm and pseudo-second-order kinetics model. More importantly, no pH adjustment was considered necessary when the ZnO/PPAC adsorbent was applied for the removal of Pb(II) ions. The negative values of ΔH° and ΔG° indicated the exothermic adsorption process and spontaneous nature of the Pb(II) adsorption process of the designated adsorbent within the temperature range. Our findings emphasize the potential of PPAC and ZnO/PPAC

adsorbents for the remediation of highly Pb-contaminated water.

Acknowledgements

Authors thank for the financial support from Lembaga Pengelola Dana Pendidikan or the Indonesia Endowment Funds for Education (LPDP) under the project Riset and Inovasi untuk Indonesia Maju (RIIM) batch 2 with contract No. 82/II.7/HK/2022 under VS. The authors also thank the Research Center for Applied Microbiology (PRMT) and Basics Advances Characterization Laboratory through e-Layanan Sains at the National Research and Innovation Agency of the Republic of Indonesia (BRIN), Analytical Chemistry Laboratory at Institut Teknologi Bandung, and the Collaborative Research Center for Zero Waste and Sustainability at UKWMS for the research facilities.

References

- [1] P.B. Tchounwou, C.G. Yedjou, A.K. Patlolla, D.J. Sutton, Heavy metal toxicity and the environment, in: Luch A., eds., *Molecular, Clinical and Environmental Toxicology, Experientia Supplementum*, vol. 101, 2012, pp. 133–164, https://doi.org/10.1007/978-3-7643-8340-4_6.
- [2] M. Koller, H.M. Saleh, Introductory chapter: introducing heavy metals, in: *Heavy Metals*, InTech, 2018, <https://doi.org/10.5772/intechopen.74783>.
- [3] R. Grigoryan, V. Petrosyan, D. Melkom Melkomian, V. Khachadourian, A. McCartor, B. Crape, Risk factors for children's blood lead levels in metal mining and smelting communities in Armenia: a cross-sectional study, *BMC Publ Health* 16 (2016) 945, <https://doi.org/10.1186/s12889-016-3613-9>.
- [4] D. O'Connor, D. Hou, J. Ye, Y. Zhang, Y.S. Ok, Y. Song, F. Coulon, T. Peng, L. Tian, Lead-based Paint remains a major public health concern: a critical review of global production, trade, use, exposure, health risk, and implications, *Environ Int* 121 (2018) 85–101, <https://doi.org/10.1016/j.envint.2018.08.052>.
- [5] M. Ramesh, R.P. Saini, Effect of different batteries and diesel generator on the performance of a stand-alone hybrid renewable energy system, *Energy Sour Part A Recov Util Environ Eff* (2020) 1763520, <https://doi.org/10.1080/15567036.2020.1763520>.
- [6] A.N. Ghanim, F.A. Al-Saadi, A hybrid system for lead removal of simulated battery industry Wastewater using electrocoagulation/electroflotation, *Separ Sci Technol* 57 (14) (2022) 2298–3311, <https://doi.org/10.1080/01496395.2022.2055576>.
- [7] W.I. Mortada, M.A. Sobh, M.M. El-Defrawy, S.E. Farahat, Study of lead exposure from automobile exhaust as a risk for nephrotoxicity among traffic policemen, *Am J Nephrol* 21 (4) (2001) 274–279, <https://doi.org/10.1159/000046261>.
- [8] A. Prabhakar, S. Mishra, A.P. Das, Isolation and identification of lead (Pb) solubilizing bacteria from automobile waste and its potential for recovery of lead from end of life waste batteries, *Geomicrobiol J* 36 (10) (2019) 894–903, <https://doi.org/10.1080/01490451.2019.1654044>.
- [9] K.K. Wong, C.K. Lee, K.S. Low, M.J. Haron, Removal of Cu and Pb from electroplating wastewater using tartaric acid modified rice husk, *Process Biochem* 39 (4) (2003) 437–445, [https://doi.org/10.1016/S0032-9592\(03\)00094-3](https://doi.org/10.1016/S0032-9592(03)00094-3).
- [10] D. Sharma, P.K. Chaudhari, N. Pawar, A.K. Prajapati, Preparation and characterization of ceramic microfiltration

- membranes for removal of cr (Vi) and pb from electroplating effluent, *Indian J Chem Technol* 27 (2020) 294–302, <https://doi.org/10.56042/ijct.v27i4.25229>.
- [11] D. Hartiningsih, S. Diana, Y. MS, M.R. Ismail, Q.W. Sari, Water quality pollution indices to assess the heavy metal contamination: a case study of the estuarine waters in Cirebon City (West Java, Indonesia) Pre- and post- CARE COVID-19, *Environ Sustain Indicat* 21 (2024) 100318, <https://doi.org/10.1016/j.indic.2023.100318>.
- [12] M. Jaishankar, T. Tseten, N. Anbalagan, B.B. Mathew, K.N. Beeregowda, Toxicity, mechanism and health effects of some heavy metals, *Interdiscipl Toxicol* 7 (2014) 60–72, <https://doi.org/10.2478/intox-2014-0009>.
- [13] A. Neisi, M. Farhadi, B. Cheraghian, A. Dargahi, M. Ahmadi, A. Takdastan, K. Ahmadi Angali, Consumption of foods contaminated with heavy metals and their association with cardiovascular disease (CVD) using GAM software (cohort study), *Heliyon* 10 (2024) e24517, <https://doi.org/10.1016/j.heliyon.2024.e24517>.
- [14] A. Dargahi, S. Rahimpouran, H.M. Rad, E. Eghlimi, H. Zandian, A. Hosseinkhani, M. Vosoughi, F. Valizadeh, R. Hossinzadeh, Investigation of the link between the type and concentrations of heavy metals and other elements in blood and urinary stones and their association to the environmental factors and dietary pattern, *J Trace Elem Med Biol* 80 (2023) 127270, <https://doi.org/10.1016/j.jtemb.2023.127270>.
- [15] K.O. Iwuozor, Prospects and challenges of using coagulation-flocculation method in the treatment of effluents, *Adv J Chem Sect A* 2 (2) (2019) 105–127, <https://doi.org/10.29088/SAMI/AJCA.2019.2.105127>.
- [16] S. Omar, M.S. Muhamad, L. Te Chuan, N.N. Rudi, N. Hamidon, N.H.A. Hamid, H. Harun, N.M. Sunar, R. Ali, Effect of hydroxyapatite (HAp) adsorbent dosage towards lead removal, *Int J Emerg Trends Eng Res* 8 (1.2) (2020) 201–205, <https://doi.org/10.30534/ijeter/2020/2881.22020>.
- [17] S. Kokate, K. Parasuraman, H. Prakash, Adsorptive removal of lead ion from water using banana stem scutcher generated in fiber extraction process, *Res Eng* 14 (2022) 100439, <https://doi.org/10.1016/j.rineng.2022.100439>.
- [18] L. Velarde, M.S. Nabavi, E. Escalera, M.L. Antti, F. Akhtar, Adsorption of heavy metals on natural zeolites: a review, *Chemosphere* 328 (2023) 138508, <https://doi.org/10.1016/j.chemosphere.2023.138508>.
- [19] S. Siddiquee, K. Rovina, S. Al Azad, Heavy metal contaminants removal from wastewater using the potential filamentous fungi biomass: a review, *J Microb Biochem Technol* 7 (6) (2015) 384–393, <https://doi.org/10.4172/1948-5948.1000243>.
- [20] M.H. Hussein, I. O. Saeed Phytoremediation, Plant synergy - bacteria for treatment of heavy metals, *J Pharm Negat Results* 13 (1) (2022) 933–941, <https://doi.org/10.47750/pnr.2022.13.s01.111>.
- [21] G. Gedda, K. Balakrishna, R.U. Devi, K.J. Shah, Introduction to conventional wastewater treatment technologies: limitations and recent Advances, in: *Advances in Wastewater Treatment I*, 2021, pp. 1–36, <https://doi.org/10.21741/9781644901144-1>.
- [22] R. Vidu, E. Matei, A.M. Predescu, B. Alhalaili, C. Pantilimon, C. Tarcea, C. Predescu, Removal of heavy metals from wastewaters: a challenge from current treatment methods to nanotechnology applications, *Toxics* 8 (2020) 101, <https://doi.org/10.3390/toxics8040101>.
- [23] P.E. Payandeh, N. Mehrdadi, P. Dadgar, Study of biological methods in landfill leachate treatment, *Open J Ecol* 7 (2017) 568–580, <https://doi.org/10.4236/oje.2017.79038>.
- [24] R. Chakraborty, A. Asthana, A.K. Singh, B. Jain, A.B.H. Susan, Adsorption of heavy metal ions by various low-cost adsorbents: a review, *Int J Environ Anal Chem* 102 (2) (2022) 342–379, <https://doi.org/10.1080/03067319.2020.1722811>.
- [25] H.M. Zwain, M. Vakili, I. Dahlan, Waste material adsorbents for zinc removal from wastewater: a Comprehensive Review, *Int J Chem Eng* 2014 (2014) 347912, <https://doi.org/10.1155/2014/347912>.
- [26] V.C. Renge, S. V. Khedkar, S. V. Pande, Removal of heavy metals from wastewater using low cost adsorbents : a review, *Scient Rev Chem Commun J* 2 (1) (2012) 173–180, <https://doi.org/10.2147/SAR.S24800>.
- [27] H.A. Hegazi, Removal of heavy metals from wastewater using agricultural and industrial wastes as adsorbents, *HBRC J* 9 (3) (2013) 276–282, <https://doi.org/10.1016/j.hbrj.2013.08.004>.
- [28] N.F. Abd Ghapar, R. Abu Samah, S. Abd Rahman, Pineapple peel waste adsorbent for adsorption of Fe(III), *IOP Conf Ser Mater Sci Eng* 991 (2020) 012093, <https://doi.org/10.1088/1757-899X/991/1/012093>.
- [29] S. Dev, A. Khamkhash, T. Ghosh, S. Aggarwal, Adsorptive removal of Se(IV) by citrus peels: effect of adsorbent entrapment in calcium alginate beads, *ACS Omega* 5 (28) (2020) 17215–17222, <https://doi.org/10.1021/acsomega.0c01347>.
- [30] M. M. A., Batch removal of hazardous safranin-O in wastewater using pineapple peels as an agricultural waste based adsorbent, *Int J Environ Monit Anal* 2 (3) (2014) 128–133, <https://doi.org/10.11648/j.ijema.20140203.11>.
- [31] T. Janani, J.S. Sudarsan, K. Prasanna, Grey water recycling with corn cob as an adsorbent, *AIP Conf Proc* 2112 (2019) 020181, <https://doi.org/10.1063/1.5112366>.
- [32] C.C.O. Alves, A.S. Franca, L.S. Oliveira, Removal of phenylalanine from aqueous solutions with thermo-chemically modified corn cobs as adsorbents, *LWT* 51 (1) (2013) 1–8, <https://doi.org/10.1016/j.lwt.2012.11.012>.
- [33] S.B. Daffalla, H. Mukhtar, M.S. Shaharun, Preparation and characterization of rice husk adsorbents for phenol removal from aqueous systems, *PLoS One* 15 (12) (2020) e0243540, <https://doi.org/10.1371/journal.pone.0243540>.
- [34] J.I. Obianyo, Characterization and removal of nickel (II) from paint industry effluent by rice husk adsorbent, *Rwanda J Eng Sci Technol Environ* 4 (1) (2021) 1–19, <https://doi.org/10.4314/rjeste.v4i1.6>.
- [35] Y. Guo, W. Zhu, G. Li, X. Wang, L. Zhu, Effect of alkali treatment of wheat straw on adsorption of Cu(II) under acidic condition, *J Chem* 2016 (2016) 6326372, <https://doi.org/10.1155/2016/6326372>.
- [36] W. Liu, X. Zhang, H. Ren, X. Hu, X. Yang, H. Liu, Co-production of spiroloxane and biochar adsorbent from wheat straw by a low-cost and environment-friendly method, *J Environ Manag* 338 (2023) 117851, <https://doi.org/10.1016/j.jenvman.2023.117851>.
- [37] J. Ma, D. Huang, J. Zou, L. Li, Y. Kong, S. Komarneni, Adsorption of methylene blue and orange II pollutants on activated carbon prepared from banana peel, *J Porous Mater* 22 (2015) 301–311, <https://doi.org/10.1007/s10934-014-9896-2>.
- [38] A. Dargahi, M.R. Samarghandi, A. Shabanloo, M.M. Mahmoudi, H.Z. Nasab, Statistical modeling of phenolic compounds adsorption onto low-cost adsorbent prepared from *Aloe vera* leaves wastes using CCD-RSM optimization: effect of parameters, isotherm, and kinetic studies, *Biomass Convers Biorefin* 13 (2023) 7859–7873, <https://doi.org/10.1007/s13399-021-01601-y>.
- [39] I. Ibrahim, T. Tsubota, M.A. Hassan, Y. Andou, Surface functionalization of biochar from oil palm empty fruit bunch through hydrothermal process, *Processes* 9 (1) (2021) 149, <https://doi.org/10.3390/pr9010149>.
- [40] S. Mamman, F.B.M. Suah, M. Raaov, F.S. Mehamod, S. Asman, N.N.M. Zain, Removal of bisphenol A from aqueous media using a highly selective adsorbent of hybridization cyclodextrin with magnetic molecularly imprinted polymer, *R Soc Open Sci* 8 (2021) 201604, <https://doi.org/10.1098/rsos.201604>.
- [41] S.K. Gebremariam, L.F. Dumée, P.L. Llewellyn, Y.F. Alwahedi, G.N. Karanikolos, Metal-organic framework hybrid adsorbents for carbon capture - a review, *J Environ Chem Eng* 11 (2023) 109291, <https://doi.org/10.1016/j.jece.2023.109291>.
- [42] G. Avci, S. Velioglu, S. Keskin, High-throughput screening of MOF adsorbents and membranes for H₂ purification and CO₂ capture, *ACS Appl Mater Interfaces* 10 (39) (2018) 33693–33706, <https://doi.org/10.1021/acsami.8b12746>.

- [43] R. Kukobat, R. Škrbić, P. Massiani, K. Baghdad, F. Launay, M. Sarno, C. Cirillo, A. Senatore, E. Salcin, S.G. Atlagić, Thermal and structural stability of microporous natural clinoptilolite zeolite, *Microporous Mesoporous Mater* 341 (2022), <https://doi.org/10.1016/j.micromeso.2022.112101>.
- [44] M.A. Zulfikar, A.R. Utami, N. Handayani, D. Wahyuningrum, H. Setiyanto, M.Y. Azis, Removal of phthalate ester compound from PVC plastic samples using magnetic molecularly imprinted polymer on the surface of superparamagnetic Fe₃O₄ (Fe₃O₄@MIPs), *Environ Nanotechnol Monit Manag* 17 (2022) 100646, <https://doi.org/10.1016/j.enmm.2022.100646>.
- [45] M. Oumam, A. Abourriche, S. Mansouri, M. Mouiya, A. Benhammou, Y. Abouliatim, Y. El Hafiane, H. Hannache, M. Birot, R. Pailler, R. Naslain, Comparison of chemical and physical activation processes at obtaining adsorbents from Moroccan oil shale, *Oil Shale* 37 (2) (2020) 139–157, <https://doi.org/10.3176/oil.2020.2.04>.
- [46] H. Albatrni, H. Qiblawey, M.J. Al-Marri, Walnut shell based adsorbents: a review study on preparation, mechanism, and application, *J Water Proc Eng* 45 (2022) 102527, <https://doi.org/10.1016/j.jwpe.2021.102527>.
- [47] K.G. Akpomie, J. Conradie, Synthesis, characterization, and regeneration of an inorganic–organic nanocomposite (ZnO@biomass) and its application in the capture of cationic dye, *Sci Rep* 10 (2020) 14441, <https://doi.org/10.1038/s41598-020-71261-x>.
- [48] B.C. Yong, A.A.A. Raman, A. Buthiyappan, M.I.L.Z. Abidin, Synthesis and characterization of sugarcane bagasse cellulose-capped silver nanoparticle using ultrasonic irradiation for the adsorption of heavy metal, *Asia Pac J Chem Eng* 15 (3) (2020) e2433, <https://doi.org/10.1002/apj.2433>.
- [49] F. Abdelghaffar, Biosorption of anionic dye using nanocomposite derived from chitosan and silver nanoparticles synthesized via cellulosic banana peel bio-waste, *Environ Technol Innov* 24 (2021) 101852, <https://doi.org/10.1016/j.eti.2021.101852>.
- [50] Z. Wang, W. Xu, F. Jie, Z. Zhao, K. Zhou, H. Liu, The selective adsorption performance and mechanism of multiwall magnetic carbon nanotubes for heavy metals in wastewater, *Sci Rep* 11 (2021) 16878, <https://doi.org/10.1038/s41598-021-96465-7>.
- [51] A. Mohammadifard, D. Allouss, M. Vosoughi, A. Dargahi, A. Moharrami, Synthesis of magnetic Fe₃O₄/activated carbon prepared from banana peel (BPAC@Fe₃O₄) and salvia seed (SSAC@Fe₃O₄) and applications in the adsorption of basic blue 41 textile dye from aqueous solutions, *Appl Water Sci* 12 (2022) 88, <https://doi.org/10.1007/s13201-022-01622-6>.
- [52] F. Mahdavian, A. Dargahi, M. Vosoughi, A. Mokhtari, H. Sadeghi, Y. Rashtbari, Enhanced removal of cefixime from aqueous solutions using Fe₃O₄@GO nanocomposite with ultrasonic: isotherm and kinetics study, *Desalination Water Treat* 280 (2022) 224–239, <https://doi.org/10.5004/dwt.2022.29111>.
- [53] Y. Kikuchi, Q. Qian, M. Machida, H. Tatsumoto, Effect of ZnO loading to activated carbon on Pb(II) adsorption from aqueous solution, *Carbon N Y* 44 (2) (2006) 195–202, <https://doi.org/10.1016/j.carbon.2005.07.040>.
- [54] P. Pourali, Y. Rashtbari, A. Behzad, A. Ahmadfazeli, Y. Poureshgh, A. Dargahi, Loading of zinc oxide nanoparticles from green synthesis on the low cost and eco-friendly activated carbon and its application for diazinon removal: isotherm, kinetics and retrieval study, *Appl Water Sci* 13 (2023) 101, <https://doi.org/10.1007/s13201-023-01871-z>.
- [55] P.P. Mahamuni, P.M. Patil, M.J. Dhanavade, M.V. Badiger, P. G. Shadija, A.C. Lokhande, R.A. Bohara, Synthesis and characterization of zinc oxide nanoparticles by using polyol Chemistry for their antimicrobial and antibiofilm activity, *Biochem Biophys Rep* 17 (2019) 71–80, <https://doi.org/10.1016/j.bbrep.2018.11.007>.
- [56] M. Antony Lilly Grace, K. Veerabhadra Rao, K. Anuradha, A. Judith Jayarani, A. Arun kumar, A. Rathika, X-Ray analysis and size-strain plot of zinc oxide nanoparticles by Williamson-Hall, *Mater Today Proc* 92 (2) (2023) 1334–1339, <https://doi.org/10.1016/j.matpr.2023.05.492>.
- [57] J. Iqbal, B.A. Abbasi, T. Yaseen, S.A. Zahra, A. Shahbaz, S.A. Shah, S. Uddin, X. Ma, B. Raouf, S. Kanwal, W. Amin, T. Mahmood, H.A. El-Serehy, P. Ahmad, Green synthesis of zinc oxide nanoparticles using *Elaeagnus angustifolia* L. Leaf extracts and their multiple *In vitro* biological applications, *Sci Rep* 11 (2021) 20988, <https://doi.org/10.1038/s41598-021-99839-z>.
- [58] G.J.F. Cruz, D. Mondal, J. Rimaycuna, K. Soukup, M.M. Gómez, J.L. Solis, J. Lang, Agrowaste derived biochars impregnated with ZnO for removal of arsenic and lead in water, *J Environ Chem Eng* 8 (2020) 103800, <https://doi.org/10.1016/j.jece.2020.103800>.
- [59] R. Rusnadi, M. Sholihah, N. Handayani, M.A. Zulfikar, Eggshell-alginate composites (EACs) as eco-friendly adsorbents for rhodamine B uptake from aqueous solutions, *Karbala Int J Modern Sci* 9 (2023) 574–583, <https://doi.org/10.33640/2405-609X.3317>.
- [60] N.G. Mostafa, A.F. Yunnus, A. Elawwad, Adsorption of Pb(II) from water onto ZnO, TiO₂, and Al₂O₃: process study, adsorption behaviour, and thermodynamics, *Adsorpt Sci Technol* 2022 (2022) 1–13, <https://doi.org/10.1155/2022/7582756>.
- [61] A. Dabizha, M. Kersten, Exothermic adsorption of chromate by goethite, *Appl Geochem* 123 (2020) 104785, <https://doi.org/10.1016/j.apgeochem.2020.104785>.
- [62] M.A. Darweesh, M.Y. Elgendy, M.I. Ayad, A.M.M. Ahmed, N.M. Kamel Elsayed, W.A. Hammad, A unique, inexpensive, and abundantly available adsorbent: composite of synthesized silver nanoparticles (AgNPs) and banana leaves powder (BLP), *Heliyon* 8 (4) (2022) e09279, <https://doi.org/10.1016/j.heliyon.2022.e09279>.
- [63] S. Chakravarty, A. Mohanty, T.N. Sudha, A.K. Upadhyay, J. Konar, J.K. Sircar, A. Madhukar, K.K. Gupta, Removal of Pb(II) ions from aqueous solution by adsorption using bael leaves (*Aegle marmelos*), *J Hazard Mater* 173 (1–3) (2010) 502–509, <https://doi.org/10.1016/j.jhazmat.2009.08.113>.
- [64] C.K. Singh, J.N. Sahu, K.K. Mahalik, C.R. Mohanty, B.R. Mohan, B.C. Meikap, Studies on the removal of Pb(II) from wastewater by activated carbon developed from tamarind wood activated with sulphuric acid, *J Hazard Mater* 153 (1–2) (2008) 221–228, <https://doi.org/10.1016/j.jhazmat.2007.08.043>.
- [65] L. Mouni, D. Merabet, A. Bouzaza, L. Belkhir, Adsorption of Pb(II) from aqueous solutions using activated carbon developed from apricot stone, *Desalination* 276 (1–3) (2011) 148–153, <https://doi.org/10.1016/j.desal.2011.03.038>.
- [66] R. Sudha, K. Srinivasan, P. Premkumar, Kinetic, mechanism and equilibrium studies on removal of Pb(II) using *Citrus limettioides* peel and seed carbon, *Res Chem Intermed* 42 (2016) 1677–1697, <https://doi.org/10.1007/s11164-015-2111-5>.
- [67] G. Wang, S. Zhang, P. Yao, Y. Chen, X. Xu, T. Li, G. Gong, Removal of Pb(II) from aqueous solutions by *Phytolacca americana* L. Biomass as a low cost biosorbent, *Arab J Chem* 11 (2018) 99–110, <https://doi.org/10.1016/j.arabjc.2015.06.011>.